2000-GT-0195
ASME Turbo 2000
Munich, Germany, May 8-11

HEAT TRANSFER AND FLOW ON THE SQUEALER TIP OF A GAS TURBINE BLADE

Gm S. Azad, Je-Chin Han
Turbine Heat Transfer Laboratory
Department of Mechanical Engineering
Texas A&M University
College Station, Texas 77843-3123

Robert J. Boyle
NASA Glenn Research Center, Cleveland, Ohio 44135

ABSTRACT

Experimental investigations are performed to measure the detailed heat transfer coefficient and static pressure distributions on the squealer tip of a gas turbine blade in a five-bladed stationary linear cascade. The blade is a 2-dimensional model of a modern first stage gas turbine rotor blade with a blade tip profile of a GE-E^3 aircraft gas turbine engine rotor blade. A squealer (recessed) tip with a 3.77% recess is considered here. The data on the squealer tip are also compared with a flat tip case. All measurements are made at three different tip gap clearances of about 1%, 1.5%, and 2.5% of the blade span. Two different turbulence intensities of 6.1% and 9.7% at the cascade inlet are also considered for heat transfer measurements. Static pressure measurements are made in the mid-span and near-tip regions, as well as on the shroud surface opposite to the blade tip surface. The flow condition in the test cascade corresponds to an overall pressure ratio of 1.32 and an exit Reynolds number based on the axial chord of 1.1×10^6. A transient liquid crystal technique is used to measure the heat transfer coefficients. Results show that the heat transfer coefficient on the cavity surface and rim increases with an increase in tip clearance. The heat transfer coefficient on the rim is higher than the cavity surface. The cavity surface has a higher heat transfer coefficient near the leading edge region than the trailing edge region. The heat transfer coefficient on the pressure side rim and trailing edge region is higher at a higher turbulence intensity level of 9.7% over 6.1% case. However, no significant difference in local heat transfer coefficient is observed inside the cavity and the suction side rim for the two turbulence intensities. The squealer tip blade provides a lower overall heat transfer coefficient when compared to the flat tip blade.

NOMENCLATURE

C Tip clearance gap
C_p Coefficient of pressure
C_x Axial chord length of the blade (8.61 cm)
h Local convective heat transfer coefficient (W/m^2K)
H Cavity depth (recess) (mm)
k Thermal conductivity of blade tip material (0.18 W/m K)
LE Leading edge of the blade
P Local static pressure
P_{avg} Averaged static pressure
P_t Total pressure at the inlet
P/S Pressure side of the blade
S/S Suction side of the blade
t Transition time for liquid crystal color change
T Thickness of the rim (mm)
TE Trailing edge of the blade
T_i Initial temperature of the blade tip surface
T_∞ Mainstream temperature of the flow
T_w Color change temperature of the liquid crystal, green-to-red
Tu Turbulence intensity level at the inlet
X Axial distance (cm)
α Thermal diffusivity of tip material (1.25×10^{-7} m^2/s)

INTRODUCTION

To achieve higher thermal efficiency and thrust modern gas turbine engines operate at high combustor outlet temperatures of 1300-1500C. Turbine blades are exposed to these high temperature gases and undergo severe thermal stress and fatigue. Blade tips are one of the most susceptible regions, because they are difficult to cool and are subject to potential damage due to the large thermal load. The hot gases flowing through the gap between the blade tip and the shroud cause this large thermal load on the blade tip. This flow sometimes called tip leakage flow, accelerates due to the pressure difference between the pressure and suction sides of the blade, which causes thin boundary layers and high heat transfer rates. This tip leakage flow is undesirable because it chips away the pressure side tip corner from the mid-chord to the trailing edge. As the blade tip is chipped away, the tip gap width increases allowing more leakage flow through the tip gap and accelerating blade tip failure. Thus, it increases the losses in the flow.

It is recognized that the blade tip geometry and subsequent tip leakage flows significantly effect the aerodynamic efficiency of turbines. The influence of tip gap on turbine efficiency is so significant that designers have a strong desire to improve the efficiency by decreasing the tip-to-shroud operating gaps, or by implementing more

effective tip clearance controls. However, it is difficult to completely seal the hot leakage flow through the tip gap. A common technique to reduce the tip leakage flow is to use a recessed tip, which is known as a squealer tip. A squealer tip allows a smaller tip clearance, without the risk of a catastrophic failure, in case the tip rubs against the shroud during turbine operation. The smaller tip gap reduces the flow rate through the tip gap, resulting in smaller losses and lower heat transfer. It is also believed that the groove (tip recess) acts as a labyrinth seal to increase flow resistance. Thus, it is important to know both the flow field and heat transfer behavior on the squealer tip of a gas turbine blade. Reliable experimental data are also important to develop and validate computational codes to predict flow and heat transfer distributions on turbine blades.

Limited information on the flow field and heat transfer on a squealer blade tip is available in the existing literature. Metzger et al. (1989) and Chyu et al. (1989) studied heat transfer on rectangular grooved tip models. They performed experiments using cavities of varying depth-to-width (width of the cavity) and tip gap-to-width (width of the cavity) ratios, and incorporated the effect of relative motion by introducing a moving shroud surface over the grooved tip model. They reported that the local heat transfer coefficient in the upstream end of the cavity is greatly reduced when compared with a rectangular flat tip, while in the downstream end of the cavity, the heat transfer coefficient is higher due to flow reattachment inside the cavity. They concluded that for a given pressure difference across the gap, there is an optimum value of depth-to-width ratio beyond which no further flow reduction will occur. They recommended shallow cavities if overall heat transfer reduction on the cavity wall is desired.

The above-cited experimental studies provide insight into the nature of the flow field and heat transfer around the cavity in a rectangular tip model case. Heyes et al. (1991) studied tip leakage on plane and squealer tips in a linear cascade environment. They reported leakage flow data on plane tip, suction side squealers, and pressure side squealers. No heat transfer data was reported. They concluded that the use of squealers, particularly, suction side squealers are more beneficial than the flat tip. Yang and Diller (1995) reported local heat transfer coefficient on a turbine blade tip model with a recessed cavity (squealer tip) in a stationary linear cascade environment. Based on the measurement at a single point on the cavity floor, they reported that the convection coefficients are insensitive of tip gap height. Ameri et al. (1997) numerically investigated the flow and heat transfer on the squealer tip of a GE-E^3 first stage gas turbine blade. They considered a smooth tip, 2% recess, and 3% recess with a 1% tip clearance for all cases. They observed higher heat transfer on the bottom of the cavity when compared with the plane tip. The heat transfer on the pressure side rim is comparable to the plane case but higher on the suction side rim. They concluded that large heat transfer on the bottom of the cavity is due to flow impingement containing hot gas.

No other experimental or numerical studies on squealer tip flow and heat transfer are available in the current literature. The existing literature, however, contains many experimental and numerical investigations on the flow field in and around turbine blade plane-tip models. Studies by Bindon and Morphus (1988) and Bindon (1989) have contributed to the general understanding of tip leakage flow patterns. Moore et al. (1989) also contributed to the understanding of the flow field through tip gaps. Yaras and Sjolander (1991) studied the effect of simulated rotation on tip leakage and found that rotation causes a significant reduction in the gap mass flow rate. Sjolander and Cao (1995) studied the flow field in an idealized turbine tip gap. Kaiser and Bindon (1997) investigated a quantitative analysis of the effects of tip clearance, tip geometry, and multiple stages on turbine stage efficiency in a rotating turbine rig environment. Other works studied the effect of tip clearances on leakage and efficiency loss prediction. Several heat transfer studies are available on turbine blade plane-tip models. Mayle and Metzger (1982) did the earliest study on rectangular plane-tip model heat transfer. Metzger et al. (1991) used several heat flux sensors to measure local tip heat fluxes on the flat tips at two different tip gaps in a rotating turbine rig. They also provided a numerical model to estimate tip and shroud heat transfer. Ameri and Steinthorsson (1995, 1996) predicted rotor blade tip and shroud heat transfer for a SSME (Space Shuttle Main Engine) turbine. Ameri et al. (1998) also predicted the effects of tip clearance and casing recess on heat transfer and stage efficiency for several squealer blade-tip geometries. Most recently, Ameri and Bunker (1999) performed a computational study to investigate detailed heat transfer distributions on the blade tip surfaces of a large power generation turbine. Bunker et al. (1999) studied the flow and heat transfer on the plane-tip in a three-blade linear cascade. Azad et al. (2000) also studied flow and heat transfer on the plane tip in a five-blade linear cascade. The plane-tip heat transfer results from Azad et al. (2000) are compared with the squealer tip results in this study.

With the development of supercomputers, numerical investigations are playing an increasingly important role in the study and design of turbine blade tip flow and heat transfer. Without reliable experimental data, however, the numerical models could not be validated and properly employed in the design and analysis of blade tip heat transfer and flow field. This study will fulfill the need for experimental heat transfer data on a gas turbine squealer blade tip. This will be the first experimental data available in the open literature with complete information on the pressure and heat transfer on the squealer tip of a gas turbine blade tip profile (GE-E^3) whose profile geometry is open to the public domain. The test section used for this study is a five-blade linear cascade, with the three middle blades having a variable tip gap, and the center blade having a squealer tip. The tip profile used here represents a first stage rotor blade tip of a modern aircraft gas turbine engine (GE-E^3). Systematic pressure measurements in the near-tip region and on the shroud surface, and heat transfer measurements on the blade-tip surface are done for a 3.77% tip recess and a tip gap clearance of 1%, 1.5%, and 2.5% of the blade span. Two inlet free-stream turbulence intensity levels are also considered. The effect of unsteady wakes, shock waves, and blade rotation, which may be important in real operating condition, is not considered here. However, it provides a basic information of heat transfer and pressure distribution on a gas turbine squealer blade tip. This data is presented in a standard format with standardized boundary conditions that could also be used by numerical people in the gas turbine community.

EXPERIMENTAL SETUP

Measurements are done in a stationary blow down facility with a five-bladed linear cascade. A detailed description of the facility is given in Azad et al. (2000). The facility is capable of maintaining a steady flow at the cascade inlet (velocity variation within $\pm$ 3%) for one-minute period. A small gap is maintained at the junction of the blade cascade and the inlet flow loop to trip the boundary layer. This location for the boundary layer trip is 26.7 cm upstream from the center blade leading edge. A turbulence-generating grid of 57% porosity is also placed at this location for high turbulence tests. The turbulence grid is composed of 12.25-mm wide square bars with 33.02 x 27.94 mm opening between bars. Hot film anemometry measurements, using a TSI IFA-100 unit, show that the free-stream turbulence intensity at a distance of 6 cm upstream from the blade leading edge is 6.1% without the turbulence grid and 9.7% with the turbulence grid. Turbulence length scale is estimated to be 1.5 cm for 9.7% turbulence case, which is slightly larger than the turbulence grid size.

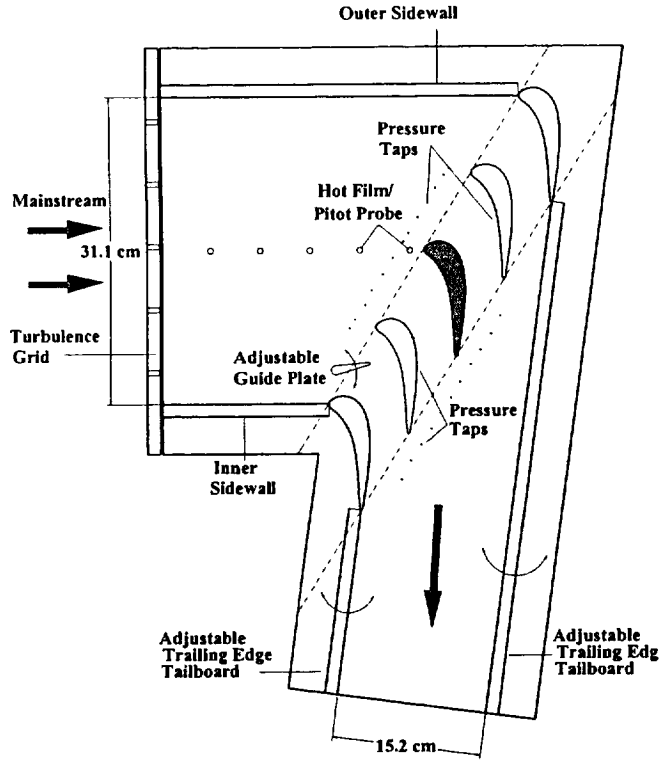

Fig. 1. Test Section with 5-Blade Cascade

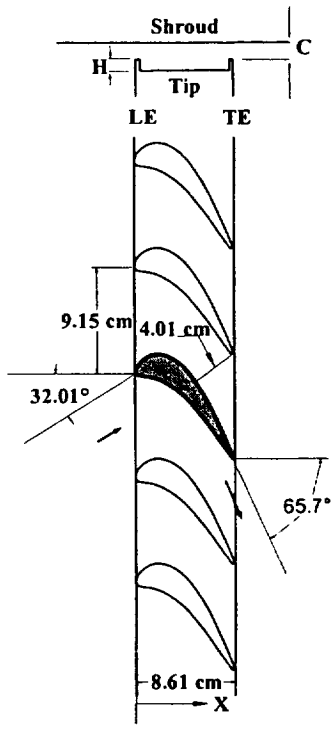

Fig. 2. Blade Tip and Shroud Definition

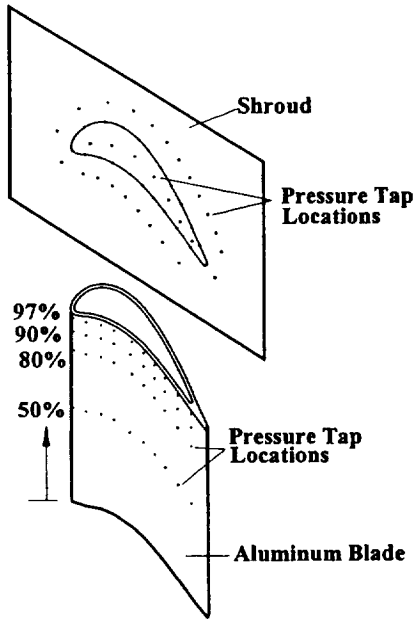

Fig. 3. Pressure Tap Locations on Blade and Shroud

The five-bladed linear cascade has 4-flow passages. The two far-end blades work as guide vanes and the outside wall, and the center blade work as a test blade. **Figure 1** shows the test cascade model. The cascade inlet dimensions are 31.1 cm wide and 12.2 cm high (span). Each blade has a 12.2 cm span and a 8.61 cm axial chord length. This dimension is three times (3X) the dimensions of a GE-E^3 blade profile. The blades are made of aluminum and are EDM machine finished. The test section's top, bottom, and sides are made of 1.27 cm thick clear Polycarbonate (Lexan); however, a 1.2 cm thick clear acrylic replaces the top cover plate (shroud) for heat transfer tests, to facilitate the best optical access to the test blade (center blade). Two separate but identical blades are used for both the pressure and heat transfer measurements.

Each blade has a constant cross section for the entire span and represents the tip section of an aerodynamic turbine blade. **Figure 2** represents the blade tip configuration in the cascade. The blade leading edge pitch (p) is 9.15 cm and the axial chord length is 8.61 cm. The throat diameter at the point of minimum distance between two blades is 4.01 cm, which, with a span of 12.2 cm, gives a throat aspect ratio of about 3. The inlet flow angle to the test blade is 32.01^0 and the exit angle is 65.7^0, giving a total turning of 97.71^0. The center blade has a 4.6 mm recess (depth of the cavity, H), which is 3.77% of the blade span (12.2 cm). A tip gap (C) is maintained between the tip and shroud surfaces as shown in **Figure 2**. The tip gaps used for this study are 1.31 mm, 1.97 mm, and 3.29 mm, which correspond to about 1%, 1.5%, and 2.5% of the blade span (12.2 cm). Hard rubber gaskets of desired thickness are placed on top of the sidewalls, the trailing edge tailboards, and the two outer guide blades to create tip gaps of desired height.

The pressure tap blade is made of aluminum with several sets of pressure taps as shown in **Figure 3.** The pressure taps are placed on both the pressure and suction surfaces. Pressure taps are also placed on the shroud surface opposite the blade tip surface to measure the pressure distribution on the shroud surface. Each pressure tap tubing has an outer and inner diameter of 1.65 mm and 1.35 mm, respectively. The tap holes (1.35 mm diameter) are located in the mid-span (50% of blade height) of the blade, at a height of 80%, 90%, and 97% of the span as measured from the base of the blade. A total of 52 pressure taps measure the shroud surface pressure. One set of pressure taps is located around the tip perimeter and along the mean camber line, and a second set of taps is located 12.52 mm outside the tip edge. No

pressure taps are placed on the tip surface. These pressure distributions are useful in estimating the tip leakage flow.

Figure 4 represents the heat transfer blade. The lower portion of the blade is made of aluminum for structural rigidity against the aerodynamic forces present during the tests. The upper portion of the blade has an inner aluminum core and an outer shell made of black polycarbonate with a low value of thermal conductivity for transient liquid crystal test. The polycarbonate tip has a 4.6 mm deep cavity and a 2.3 mm thick rim. The base thickness of the polycarbonate shell underneath the cavity is 6.35 mm and the wall that surrounds the inner aluminum core has a thickness of 3.175 mm. The polycarbonate shell is closely fitted with the inner aluminum core. The shell is also glued to the inner core through the rim contact surface for better rigidity. Three cartridge heaters are embedded into the inner core. The cartridge heaters provide heating to the aluminum core, which in turn heats the outer polycarbonate shell. The blade is fastened to the bottom endwall with screws.

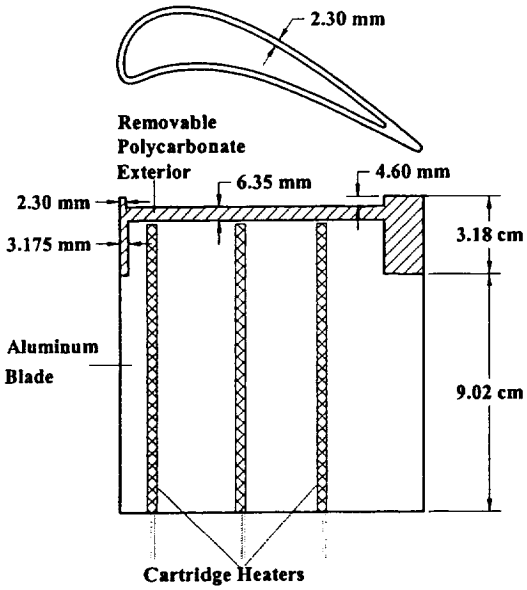

Fig. 4. Heat Transfer Blade

The usual operating condition for this cascade is set at an inlet total pressure of 143 kPa, an exit average static pressure of 108.3 kPa, which gives an overall blade pressure ratio of 1.32. The mass flow rate through the cascade is about 5.9 kg/s. During the blow down test, the inlet air velocity is kept at about 85 m/s; the exit air velocity at 199 m/s, and the corresponding Reynolds number of 1.1×10^6 based on axial chord length and exit flow velocity. The corresponding Mach numbers at the inlet and exit are 0.25 and 0.59, respectively.

FLOW CONDITION IN THE CASCADE AND PRESSURE MEASUREMENT

The flow patterns at the cascade inlet and exit plane, and through the suction and pressure side passages of the test blade are measured. The detailed measurement is described in Azad et al. (2000). The inlet and exit flow pattern is represented by the coefficient of pressure (C_p). The coefficient of pressure is defined as:

$$C_p = \frac{P_t - P}{P_t - P_{avg}}$$

Here, P_{avg} is the average static pressure as measured by the inlet (or exit) plane pressure taps, P_t is the total inlet pressure, and P is the local static pressures as measured by the inlet (or exit) pressure taps. This C_p actually represents a non-dimensional velocity field, which is important for a quick review of the velocity field pattern. **Figure 5a** represents the C_p at the cascade inlet and the exit plane. The measurement planes are selected upstream from the leading edge and downstream from the trailing edge at a distance of 25% of the blade span. The axial distance is measured from the outermost tap location towards the innermost tap

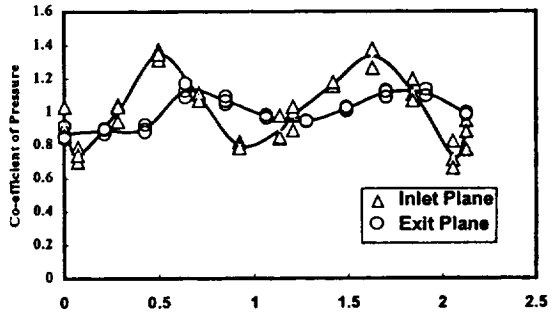

Fig. 5a. Co-efficient of Pressure at Inlet and Exit Plane

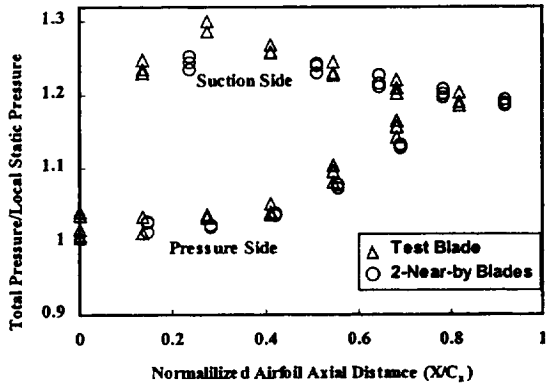

Fig. 5b. Pressure Distribution at Mid-span on the Test Blade and 2-Near-by Blades

(cascade outer and inner sidewalls are labeled in **Figure 1**). **Figure 5b** shows pressure distributions at a 50% height of the blade span on the center blade and the two nearby blades. For **Figure 5b**, the local axial position is normalized by the axial chord length. The multiple data points in **Figures 5a** and **b** represent the variation in repeated tests. The result shows that the flow patterns in the two passages are almost identical.

Static pressures are also measured at 80%, 90%, and 97% height of the blade span on both the P/S and S/S, and also on the shroud surface. Pressures are recorded with a 48-channel Scanivalve System coupled with LabView 5.0 software. LabView discarded all data that fell outside the initial mean ± 1.5 standard deviation. It then recorded the mean value of the screened data. Every pressure measurement is repeated at least three times to reduce operating uncertainty and to verify the repeatability of the data. The blow down facility is capable of giving a steady flow (the velocity variation is within $\pm$ 3%) for about one minute. The scanivalve can step through all 48 channels in this one

minute to capture the pressure data. **Figure 6** shows the ratio of the total to local static pressure distributions on the P/S and the S/S at different height of blade span for 1.97 mm (1.5% of the span) tip gap and inlet Tu =6.1% only. The ratio of pressure distribution (P_t/P) is presented as a function of normalized axial distance (X/C_x). A higher value of P_t/P corresponds to a lower static pressure, while a lower value corresponds to a higher static pressure. The static pressure difference between the P/S and the S/S is the main driving force for the leakage flow. **Figure 6** clearly shows that the maximum static pressure-difference occurs at a distance of 20-30% of the axial chord from the leading edge at 50% of the blade span. This location of maximum pressure difference has shifted toward the TE at 97% of the blade span, and the maximum static pressure difference occurs at about 40-50% of the axial chord from the LE. This shift is because of the leakage flow through the tip gap.

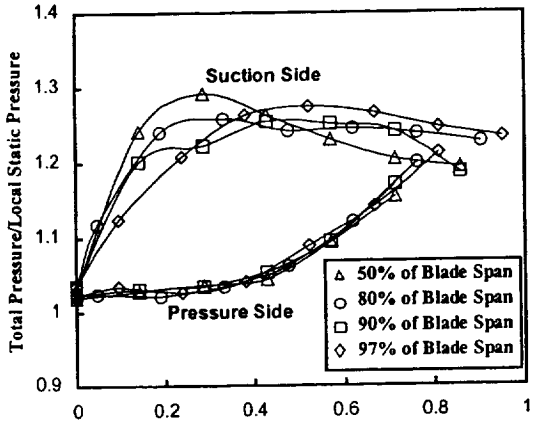

Fig. 6. Pressure Distributions From Mid-span to Near-Tip Locations for C=1.5% and Tu=6.1%

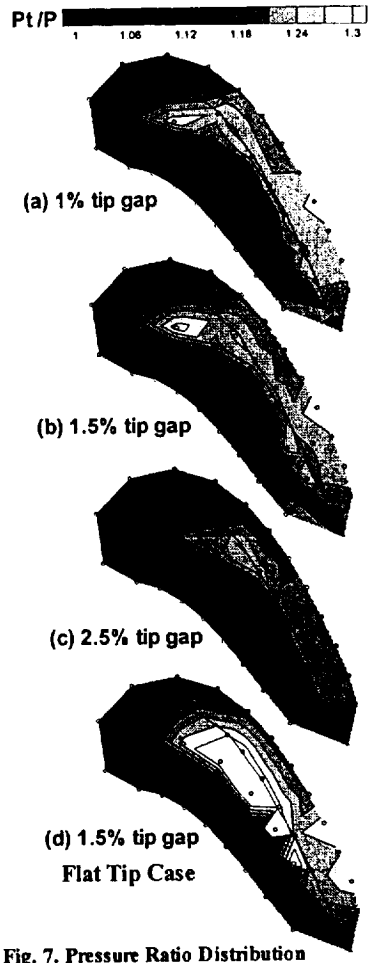

Fig. 7. Pressure Ratio Distribution on the Shroud Surface

Figures 7a, b, c, and **d** show the ratio of total to local static pressures (P_t/P) contours on the shroud surface for three different tip gaps at Tu = 6.1%. **Figures 7a, b,** and **c** are for the squealer tip at 1%, 1.5%, and 2.5% tip gap, while **7d** is for the flat tip at 1.5% tip gap. This contour plot helps explain the heat transfer results on the tip surface. The small circles on the contour plots represent the pressure tap locations relative to the tip. The pressure taps along the tip perimeter are connected by a line to indicate the tip dimension. A smaller P_t/P value means higher static pressure, while a larger value means a lower static pressure. This pressure ratio distribution clearly demonstrates the tip leakage flow path. The lower P_t/P value on the P/S indicates that the leakage flow enters the tip gap at this location, while the higher P_t/P value on the S/S indicates that the leakage flow exits the tip through this location. The flow situation in the squealer tip case represents a flow field inside a cavity. In the flow path through the tip gap, a separation vortex generates as the flow separates at the pressure side rim. The flow reattaches inside the cavity and separates again when exiting through the suction side rim. Ameri et al. (1997) also predicted this phenomenon.

The flat tip case in **Figure 7d** shows a higher value of P_t/P near the mid-suction side, which indicates a very low static pressure in this region. For the same tip gap, the squealer tip in **Figure 7b** shows a much higher static pressure. This means that the leakage flow rate through the flat tip gap is higher than the squealer tip for the same tip gap. The flat tip case also shows that the lower static pressure extends toward the trailing edge through the camber line, thus leading the flow toward the trailing edge. However, the lower static pressure occurs toward the suction side near the leading edge in the squealer tip. Thus, the leakage-flow direction shifts toward the leading edge. This may result in a higher heat transfer coefficient in the cavity toward the leading edge than the flat tip case. There is not much apparent difference between the pressure distributions at the 1% and 1.5% tip gaps as shown in Figures 7a and b. However, an appreciable difference is observed between 1% and 2.5% tip gaps.

HEAT TRANSFER MEASUREMENT AND RESULTS

A threshold intensity method of transient liquid crystal technique is used. The liquid crystals used in this study are wide band 30 to 35C crystals made by Hallcrest (R30C5W). The blade tip surface is initially coated with a thin layer of thermochromic liquid crystals, and the blade is fastened in the test cascade with the top acrylic cover in place. The cartridge heaters are turned on for three hours. The cartridge heaters heat the inner aluminum core of the test blade, and the aluminum core, in turn, heats the polycarbonate shell to a desired steady initial temperature of about 60C. The tip cavity and rim surface initial temperatures are measured by thermocouples placed at twenty-five (25) discrete locations. Two thermocouples are also placed on the suction and pressure side near-tip region toward the trailing edge. These two thermocouples work as a reference to check the initial tip surface temperature during the heat transfer test. This process of heating the blade and measuring the initial temperature is repeated several times before the final heat transfer test to ensure repeatability of the recorded

initial temperature. The initial temperature is very uniform (within 2C) throughout the tip cavity surface, except near the trailing edge region and the rim. These temperatures are then interpolated to get an initial temperature map on the whole surface. For heat transfer test, the thermocouples from the tip surface are removed. The blade is then washed and re-sprayed with liquid crystals. The blade is put back in the cascade and the cartridge heaters are turned on for three hours as before. A region of interest (ROI) is selected and a background light intensity is corrected based upon the lighting conditions on the ROI. This region of interest (ROI) is the data collection region. The system is ready for the blow down test once the lighting, threshold, and initial temperature are set. One test is done per day in a controlled environment (test cell doors are closed and the room temperature is controlled). The reference thermocouples check the initial surface temperature during a heat transfer test. Each heat transfer test is done at a preset flow condition at which the pressure measurement is made. Precise coordination of the image processing system and the flow is critical, since the heat transfer experiments are performed at transient conditions. Thermocouples placed at the cascade inlet provide the free-stream temperature, which is about 24C. The blade surface color change is monitored using an image processing system. The camera captures the color change transition time from green to the onset of red through Optimas 3.0, an image processing software. The same software translates the captured image into a data file. The test duration is small enough (~10-30 sec.) to consider a semi-infinite solid assumption. The local heat transfer coefficient on the blade tip surface is then calculated, assuming a one-dimensional transient conduction into a semi-infinite solid surface with a convective boundary condition using the following equation:

$$\frac{T_w - T_i}{T_\infty - T_i} = 1 - \exp\left(\frac{h^2 \alpha t}{k^2}\right) erfc\left(\frac{h\sqrt{\alpha t}}{k}\right)$$

Here, T_w (30C), T_i (60C), T_∞ (24C), t (~10-30 sec), k (0.18 W/m K), and α are known. The experimental uncertainty is measured using the methods of Kline and McClintock (1953). The uncertainty of the local heat transfer coefficient measured by this method is estimated to be ± 7.9 % or less. This uncertainty estimation does not include the effect of 2-dimensionality near the edges. Note that the acrylic blade material (polycarbonate) has a very low thermal conductivity of 0.18 W/m K. The liquid crystal color change transition occurs at the surface, which is kept at a uniform initial temperature. The test duration is also smaller (~10-30 sec) than the time required for the temperature to penetrate the full thickness of the insulating acrylic material. Thus, a 1-D transient, semi-infinite solid assumption is valid throughout the surface, except near the edges. Due to this 1-D assumption, the results at the tip edges are less reliable, and may suffer more uncertainty than the reported value because of the existing two-dimensional conduction effect.

The heat transfer coefficient measurements are done for the three cases of tip gaps and at two different turbulence intensities. The local heat transfer coefficient distributions for the squealer tip are presented in **Figures 8a** through **c**. For comparison, the result from Azad et al. (2000) for the flat tip case at 1.5% tip gap is also presented in **Figure 8d**. The distribution clearly shows various regions of low and high heat transfer coefficients on the tip cavity and rim surface. The magnitude of the heat transfer coefficient varies from 350 to 1150 W/m^{2}K inside the cavity and on the trailing edge portion downstream of the cavity. However, the heat transfer coefficient on the rim is much higher at about 1100 to 1700 W/m^{2}K. We present the plots in the range of 400-1100 W/m^{2}K to clearly distinguish different lower and higher heat transfer zones inside the cavity. The average heat transfer coefficient values on the rim are presented separately in a line plot to show the magnitude of the heat transfer coefficient on the rim. The flat tip result in **Figure 8d** shows that a very low heat transfer coefficient region exists near the leading edge suction side. In the mid-chord region, the heat transfer coefficient is higher toward the pressure side than the suction side, while the trailing edge has a lower heat transfer coefficient. Upon comparison of the flat tip result of **Figure 8d** with the squealer tip result in **Figure 8b** for the same tip gap, a higher local heat transfer coefficient is observed on the bottom of the cavity toward the leading edge. The local heat transfer coefficient in the trailing edge region is also higher than the flat tip case. The heat transfer coefficient on the pressure side rim is comparable to the flat tip case, while the suction side rim shows a higher heat transfer coefficient than the flat tip case. On the cavity bottom, the heat transfer coefficient is higher in the upstream-central region; however, it is much lower in the mid-chord region toward the pressure side and downstream-end of the cavity toward the trailing edge. A recirculating dead-flow zone is observed far downstream at the end of the cavity surface. Leakage flow may be entrapped in this narrow region, which causes the heat transfer coefficient to be the lowest in this region. The leakage flow may have an impingement effect on the cavity surface. It separates on the pressure side rim and may reattach inside the cavity surface. Thus, a higher heat transfer coefficient is observed on the central upstream region of the cavity bottom. The high heat transfer on the rim may be due to the flow entrance and exit effect. The leakage spills out of the cavity and exit through the suction side rim and the trailing edge. This may cause more mixing, resulting in a higher heat transfer coefficient in the suction side rim and the trailing edge than the flat tip case.

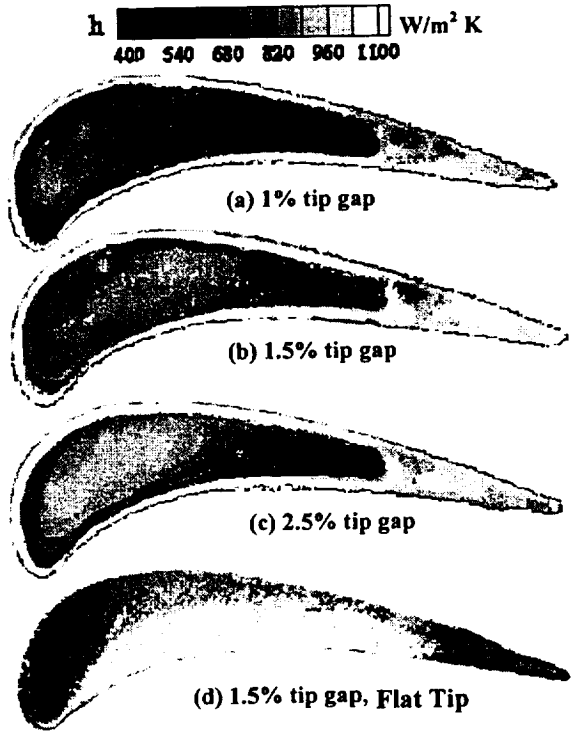

Fig. 8. Heat Transfer Coefficient at Tu = 6.1%

The effect of tip gap from 1.5% to 1% and 2.5% is reflected in **Figures 8a** and **c**. This figure clearly shows that the tip gap has a significant effect on the local heat transfer coefficient. A larger tip gap

results in an overall higher heat transfer coefficient, while a smaller tip gap results in a lower heat transfer coefficient. This is because a larger tip gap increases the amount of tip leakage flow, while a smaller tip gap decreases it.

The effect of inlet turbulence intensity from 6.1% to 9.7% is shown in **Figures 9a** through **d.** The flat tip result in **Figure 9d** at 9.7% turbulence intensity shows a similar trend but a higher magnitude of heat transfer coefficient than the 6.1% turbulence case, as shown in **Figure 8d.** The squealer-tip results in **Figures 9a** through **c** at 9.7% turbulence intensity show a similar heat transfer distribution trend as that in **Figures 8a through c** at the low turbulence level of 6.1%. The magnitude of the heat transfer coefficient at the cavity bottom is almost the same as in the low turbulence case of 6.1%. The cavity rim and the trailing edge region, however, show a higher value. A higher turbulence does not increase the magnitude of the tip leakage; however, it increases the flow fluctuations. The tip gap from 1.5% to 1% and 2.5% has an effect similar to that in the low turbulence case. However, the turbulence effect is more prominent at the larger tip gap of 2.5%.

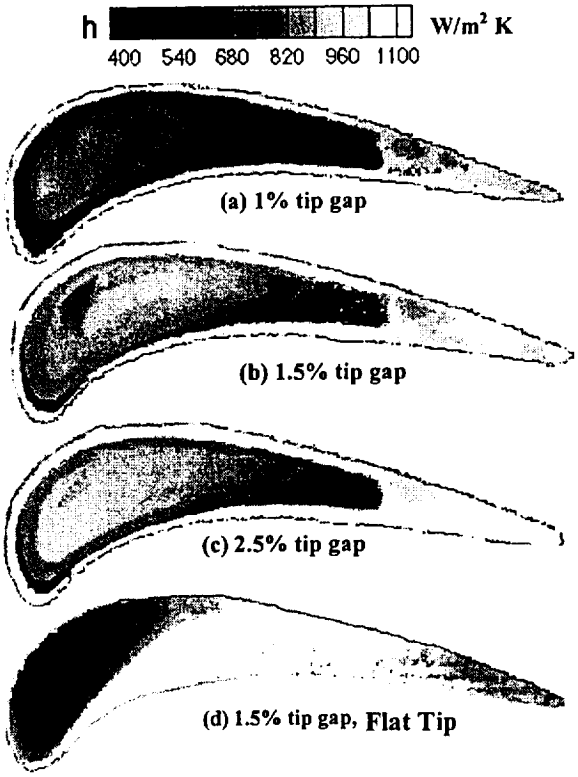

Fig. 9. Heat Transfer Coefficient at Tu = 9.7%

No experimental data is available in the literature to compare with this result, except for those of Metzger et al. (1989) rectangular tip model cavity heat transfer data. Metzger et al. (1989) found very high heat transfer coefficient on the rim of the upstream (pressure side) and downstream wall (suction side), and these have the same magnitude as in the rectangular flat tip surface. They reported a low heat transfer coefficient on the bottom of the cavity compared to the rectangular flat tip case. The cavity midfloor showed higher heat transfer coefficient than the upstream and downstream end of the cavity. Ameri et al (1997) presented a numerical heat transfer result on the squealer tip of a full rotating GE-E^3 blade for a 2% and 3% cavity recess with a 1% tip gap case. They observed that the heat transfer on the bottom of the cavity is higher than the flat (smooth) tip case. The pressure side rim showed a similar level, but the suction side rim showed a higher level of heat transfer when compared with the flat tip case. The trend of our experimental data agrees well with Ameri's et al. (1997) predicted results. It also agrees somewhat with Metzger's et al. (1989) data. We observed that at the bottom of the cavity, toward the central upstream region, the heat transfer coefficient is higher compared to the flat tip case, while it is much lower toward the downstream region and pressure side of the cavity bottom. The pressure side of the cavity rim shows a similar level of heat transfer coefficient compared with the flat tip case, while the suction side rim and the blade trailing edge region show higher heat transfer coefficients when compared with the flat tip case. The heat transfer coefficient in the front-central portion of the cavity is higher than the surrounding area and the trailing side of the cavity.

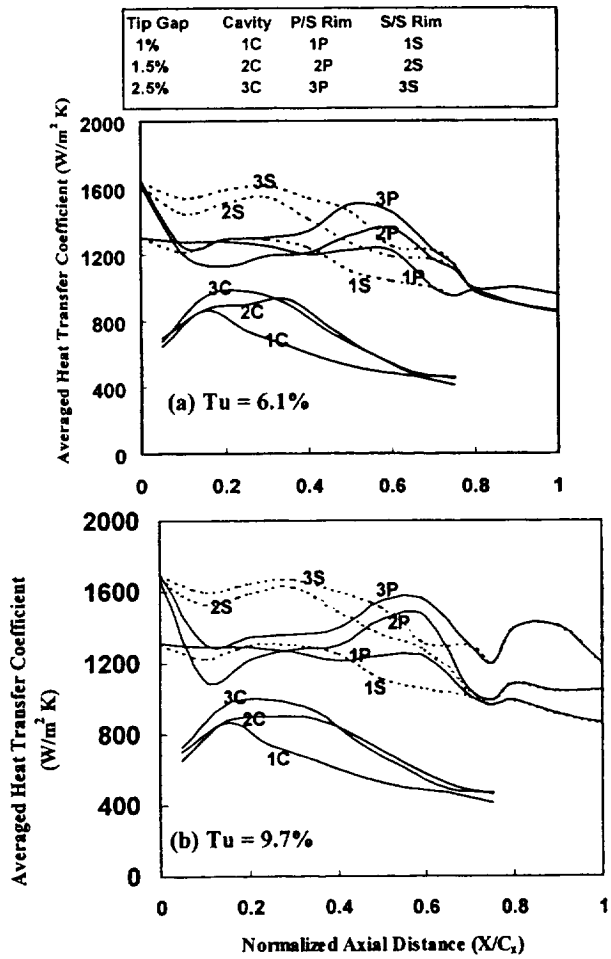

Fig. 10. Averaged Heat Transfer Coefficient at (a) Tu = 6.1%, (b) Tu = 9.7%

The averaged heat transfer coefficients are presented in **Figures 10a and b** for the three different tip gaps and at 6.1% and 9.7% turbulence intensities, respectively. The averaged heat transfer coefficient is calculated and plotted as a function of normalized axial distance from the leading edge. The result shows that the heat transfer coefficient inside the cavity and on the rim increases with tip clearance. For each tip gap case, the heat transfer coefficient inside the cavity initially increases slightly along the axial chord, then levels off and

decreases toward the downstream edge. The highest heat transfer coefficient is observed on the rim at the leading edge. The heat transfer coefficient on the suction side rim is higher up to the mid-chord than the pressure side rim, the pressure side rim then shows a higher heat transfer coefficient than the suction side rim. Turbulence has a greater effect on the pressure side rim and the trailing edge than the cavity. As seen in **Figure 10b**, this effect is prominent at larger tip clearances.

CONCLUSIONS

This study investigated the effect of tip gap and inlet turbulence intensity on detailed local heat transfer coefficient on the squealer tip surface of a gas turbine blade. The result is also compared with the flat tip case. The blade tip model is a 2-dimensional profile of an E^3 blade of an aircraft gas turbine engine with a 3.77% cavity recess. A transient liquid crystal technique is used to detail heat transfer measurements. Pressure distributions in the near tip region and on the shroud surface provide complementary information explaining the local heat transfer behavior on the tip surface in a five-blade stationary linear cascade. A typical operating condition having a Reynolds number based on airfoil axial chord and an exit velocity of 1.1×10^6 and an overall pressure ratio of 1.32 is used to measure the pressure and heat transfer coefficients. The major findings are:

1) Detailed measurements provide a better understanding of the local heat transfer behavior on the blade tip surface.
2) The pressure measurements in the near tip and on the shroud surface provide complementary information of the tip leakage flow pattern. This pressure data provides a basis for determining the tip leakage flow, and it also explains the heat transfer results. This detailed pressure and heat transfer measurement also provides a reference for further experimental or computational study.
3) Different heat transfer regions exist on the cavity surface. The front-central portion of the cavity surface contains a high heat transfer region, while a low heat transfer region exists around this region and toward the downstream of the cavity.
4) A higher heat transfer coefficient exists on the rim surface because of the entrance and exit effect. The trailing edge region also contains a high heat transfer coefficient.
5) A larger tip gap results in a higher heat transfer coefficient, while a smaller tip gap results in a lower heat transfer coefficient. This is because a larger tip gap increases the magnitude of the tip leakage flow, while a smaller tip gap decreases it.
6) An increase in the inlet turbulence intensity level from 6.1% to 9.7% slightly increases the heat transfer coefficient along the pressure side rim and the trailing edge region.
7) The heat transfer coefficient in a squealer tip is higher near the central upstream end of the cavity and the trailing edge region, while it is much lower in the mid-chord toward the pressure side and downstream end of the cavity when compared to the flat tip case. The Squealer tip cavity rim has the same level of heat transfer coefficient on the pressure side but a higher heat transfer coefficient on the suction side when compared to the flat tip case. However, the squealer tip provides an overall lower heat transfer coefficient when compared to the flat tip case.

ACKNOWLEDGEMENT

This work is prepared with the support of the NASA Glenn Research Center under grant number NAG3-2002. The NASA technical team is Mr. Robert Boyle and Dr. Raymond Gaugler. Their support is greatly appreciated. Technical discussions with Dr. C. Pang Lee of GE Aircraft Engines, Dr. Ron Bunker of GE R&D Center, and Dr. Srinath Ekkad of Louisiana State University were helpful and are acknowledged. Dr. C. Pang Lee also provided us the E^3 profile for the plane and squealer tips. His help is also appreciated.

REFERENCES

Ameri, A.A. and Bunker, R.S., 1999, "Heat Transfer and Flow on the First Stage Blade Tip of a Power Generation Gas Turbine: Part 2: Simulation Results," ASME 99-GT-283.

Ameri, A.A. and Steinthorsson, E., 1995, "Prediction of Unshrouded Rotor Blade Tip Heat Transfer," ASME 95-GT-142.

Ameri, A.A. and Steinthorsson, E., 1996, "Analysis of Gas Turbine Rotor Blade Tip and Shroud Heat Transfer," 96-GT-189.

Ameri, A.A., Steinthorsson, E. and Rigby, L. David, 1997, "Effect of Squealer Tip on Rotor Heat Transfer and Efficiency," ASME 97-GT-128

Ameri, A.A., Steinthorsson, E. and Rigby, L. David, 1998, "Effects of Tip Clearance and Casing Recess on Heat Transfer and Stage Efficiency in Axial Turbines," ASME 98-GT-369.

Azad, G. S., Han, J.C., Teng, S., and Boyle, R., 2000, "Heat Transfer and Pressure Distributions on a Gas Turbine Blade Tip," ASME 2000-GT-0194.

Bindon, J.P., 1989, "The Measurement and Formation of Tip Clearance Loss," ASME Journal of Turbomachinery, Vol. 111, pp. 258-263.

Bindon, J.P. and Morphus, G., 1988, "The Effect of Relative Motion, Blade Edge Radius and Gap Size on the Blade Tip Pressure Distribution in an Annular Turbine Cascade with Clearance," ASME 88-GT-256.

Bunker, R.S., Baily, J.C. and Ameri, A.A., 1999, "Heat Transfer and Flow on the First Stage Blade Tip of a Power Generation Gas Turbine: Part 1: Experimental Results," ASME 99-GT-169

Chyu, M.K., Moon, H.K. and Metzger, D.E., 1989, "Heat Transfer in the Tip Region of Grooved Turbine Blades," Journal of Turbomachinery, Vol. 111, pp. 131-138.

Heyes, F.J.G., Hodson, H.P., and Dailey, G.M., 1991, "The Effect of Blade Tip Geometry on the Tip Leakage Flow in Axial Turbine Cascades," ASME 91-GT-135.

Kaiser, I. and Bindon, J.P., 1997, "The Effect of Tip Clearance on the Development of Loss Behind a Rotor and a Subsequent Nozzle," ASME 97-GT-53.

Kline, S.J. and McClintock, F.A., 1953, "Describing Uncertainties in Single Sample Experiments," Mechanical Engineering, Vol. 75.

Mayle, R.E. and Metzger D.E., 1982, "Heat Transfer at the Tip of an Unshrouded Turbine Blade" Proc. Seventh Int. Heat Transfer Conf., Hemisphere Pub., pp 87-92.

Metzger, D.E., Bunker, R.S. and Chyu, M.K., 1989, "Cavity Heat Transfer on a Transverse Grooved Wall in a Narrow Flow Channel," Journal of Heat Transfer, Vol. 111, pp. 73-79.

Metzger, D.E., Dunn, M.G. and Hah, C., 1991, "Turbine Tip and Shroud Heat Transfer," Journal of Turbomachinery, Vol. 113, pp. 502-507.

Moore, J., Moore, J.G., Henry, G.S. and Chaudhury, U., 1989, "Flow and Heat Transfer in Turbine Tip Gaps," Journal of Turbomachinery, Vol. 111, pp. 301-309.

Sjolander, S. A. and Cao, D., 1995, "Measurements of the Flow in an Idealized Turbine Tip Gap," Journal of Turbomachinery, Vol. 117, pp. 578-584.

Yang, T.T. and Diller, T.E., 1995, "Heat Transfer and Flow for a Grooved Turbine Blade Tip in a Transonic Cascade," ASME-95-WA/HT-29.

Yaras, M.I. and Sjolander, S.A., 1991, "Effects of Simulated Rotation on Tip Leakage in a Planar Cascade of Turbine Blades, Part I-Tip Gap Flow," ASME 91-GT-127.